28th AIAA Applied Aerodynamics Conference
28 June - 1 July 2010, Chicago, Illinois

AIAA 2010-4375

Reduced-Order Models for the Aeroelastic Analysis of Ares Launch Vehicles

Walter A. Silva*

Veer N. Vatsa†

Robert T. Biedron‡
NASA Langley Research Center, Hampton, VA

This document presents the development and application of unsteady aerodynamic, structural dynamic, and aeroelastic reduced-order models (ROMs) for the ascent aeroelastic analysis of the Ares I-X flight test and Ares I crew launch vehicles using the unstructured-grid, aeroelastic FUN3D computational fluid dynamics (CFD) code. The purpose of this work is to perform computationally-efficient aeroelastic response calculations that would be prohibitively expensive via computation of multiple full-order aeroelastic FUN3D solutions. These efficient aeroelastic ROM solutions provide valuable insight regarding the aeroelastic sensitivity of the vehicles to various parameters over a range of dynamic pressures.

Note To Readers

The predicted performance and certain other features and characteristics of the Ares I and Ares I-X launch vehicles are defined by the U.S. Government to be Sensitive but Unclassified (SBU). Therefore, details have been removed from all plots and figures.

Introduction

AT present, the development of CFD-based reduced-order models (ROMs) is an area of active research at several government, industry, and academic institutions.[1–7] Development of ROMs based on the Volterra theory is one of several ROM methods currently under development.[8–12]

Silva and Bartels[4] introduced the development of linearized, unsteady aerodynamic state-space models for prediction of flutter and aeroelastic response using the parallelized, aeroelastic capability of the CFL3Dv6 code. The results presented provided an important validation of the various phases of the ROM development process. In Silva and Bartels,[4] the Eigensystem Realization Algorithm (ERA),[13] which transforms an impulse response (one form of ROM) into state-space form (another form of ROM), was applied for the development of the aerodynamic state-space models. The ERA is part of the SOCIT (System/Observer/Controller Identification Toolbox). Flutter results for the AGARD 445.6 Aeroelastic Wing using the CFL3Dv6 code were presented as well, including computational costs. Unsteady aerodynamic state-space models were generated and coupled with a structural model within a MATLAB/SIMULINK[14] environment for rapid calculation of aeroelastic responses including the prediction of flutter. Aeroelastic responses computed directly using the CFL3Dv6 code showed excellent comparison with the aeroelastic responses computed using the CFD-based ROM.

A primary purpose of this effort is to provide the Ares I-X flight test and the Ares I crew launch vehicle projects with cost-effective analyses that provide insight into the aeroelastic behavior of this class of launch vehicles. The present analysis develops and applies aeroelastic ROMs that are based on CFD aeroelastic analyses that fully couple the flow field and the structural flexibility. These aeroelastic ROMs are generated at each Mach number of interest along the flight trajectory and are valid for a limited range of vehicle deformations and a range of dynamic pressures at that Mach number. Due to the nature of launch vehicles, the mode shapes and frequencies of the vehicles are different at each Mach number of interest. The application of ROMs for aeroelastic analyses can yield significant computational efficiency over the more traditional method using full-order CFD aeroelastic solutions.

The resultant aeroelastic ROMs are in a state-space format suitable for use by other disciplines. Therefore, a secondary purpose of this effort is to provide the Guidance, Navigation, and Control group with ROMs that may be suitable for inclusion into their full

*Senior Research Scientist, Aeroelasticity Branch, AIAA Associate Fellow.
†Senior Research Scientist, Computational Aerosciences Branch, AIAA Associate Fellow.
‡Senior Research Scientist, Computational Aerosciences Branch, AIAA Senior Member.

ascent vehicle simulation. The use of ROMs within this simulation would provide insight regarding the dynamic aeroelastic response of the vehicle along trajectory flight conditions.

Description of CFD and System Identification Methods

The following subsections briefly describe the aeroelastic version of the FUN3D code[15] and the system identification methods used in the ROM development process.

FUN3D Code and Grid

The development of ROMs is based on the use of the FUN3D code (version 10.5) to compute the flowfield. FUN3D is a parallel, unstructured computational fluid dynamics code that supports meshes containing any combination of hexahedra, tetrahedra, prisms, and pyramids. The code is a node centered finite volume Euler and Navier-Stokes flow solver that includes the Spalart-Allmaras (SA), the Menter shear stress transport (SST), the Wilcox k-omega and the Abid k-epsilon turbulence models. In the present computations the SA and the SST models have been used. The code has various options for computing the inviscid flux quantities across volume faces, namely the van Leer flux vector splitting, the Roe flux difference splitting, the HLLC, the AUFS, LDFSS and central differencing. In the present computations the Roe flux difference splitting was used. Several flux limiters are also available such as the minmod Barth, Venkatakrishnan, van Leer, van Albada and the smooth limiter. For the present computations below Mach 0.9 no limiter was used and at Mach 0.9 and above the minmod limiter was used. The present computations have been performed on the NASA Advanced Supercomputing (NAS) RTJones and Columbia systems and the NASA Langley Research Center K cluster. The grids were partitioned among 240 processors.

The baseline unstructured mesh had 23 million nodes. This size baseline mesh was chosen based on experience performing steady CFD for the Ares I project with FUN3D. Figure 1 is an image of the Ares I vehicle and Figure 2 is an image of the forward portion of the Ares I with a sample surface grid.

The FUN3D code can be used to generate unsteady aerodynamic responses (generalized aerodynamic forces or GAFs) via the forcing of the mode shapes. This is the process that is used for the generation of the unsteady aerodynamic ROM. The FUN3D code can also be used to generate aeroelastic responses as iterations between the unsteady aerodynamics and the modal structural model. These aeroelastic responses from the FUN3D code are referred to as full aeroelastic responses.

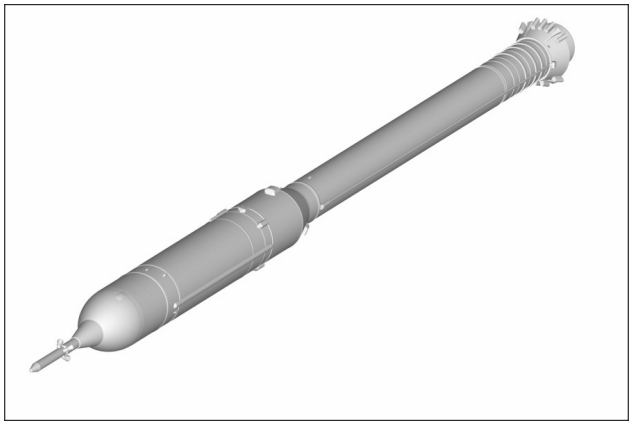

Fig. 1 Image of Ares I.

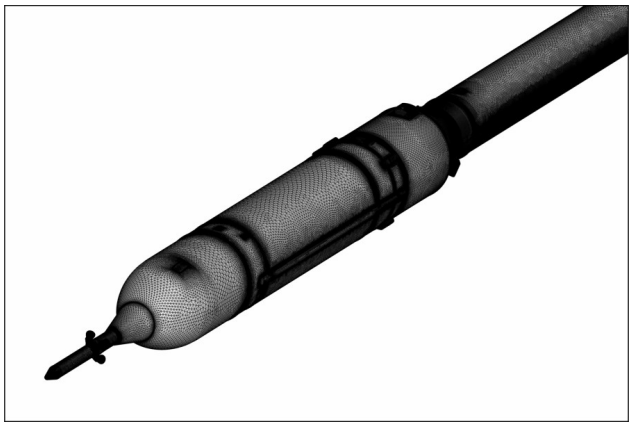

Fig. 2 Image of forward portion of Ares I with sample surface grid.

System Identification Method

The development of discrete-time state-space models that describe the modal dynamics of a structure has been enabled by the development of algorithms such as the Eigensystem Realization Algorithm (ERA)[13] and the Observer Kalman Identification (OKID)[16] Algorithm. These algorithms perform state-space realizations by using the Markov parameters (discrete-time impulse responses) of the systems of interest. These algorithms have been combined into one package known as the System/Observer/Controller Identification Toolbox (SOCIT)[17] developed at NASA Langley Research Center.

There are several algorithms within the SOCIT that are used for the development of unsteady aerodynamic discrete-time state-space models. The PULSE algorithm is used to extract individual input/output impulse responses from simultaneous input/output responses. For a four-input/four-output system, simultaneous excitation of all four inputs[1] yields four output responses. The PULSE algorithm is used to extract the individual sixteen (four times four) impulse responses that associate the response in one of the outputs due to one of the inputs. Details of the PULSE

algorithm are provided in the references. Once the individual sixteen impulse responses are available, they are then processed via the Eigensystem Realization Algorithm (ERA) in order to transform the sixteen individual impulse responses into a four-input/four-output, discrete-time, state-space model. A brief summary of the basis of this algorithm follows.

A finite dimensional, discrete-time, linear, time-invariant dynamical system has the state-variable equations

$$x(k+1) = Ax(k) + Bu(k) \tag{1}$$

$$y(k) = Cx(k) + Du(k) \tag{2}$$

where x is an n-dimensional state vector, u an m-dimensional control input, and y a p-dimensional output or measurement vector with k being the discrete time index. The transition matrix, A, characterizes the dynamics of the system. The goal of system realization is to generate constant matrices (A, B, C) such that the output responses of a given system due to a particular set of inputs is reproduced by the discrete-time state-space system described above.

For the system of Eqs. (1) and (2), the time-domain values of the systems discrete-time impulse response are also known as the Markov parameters and are defined as

$$Y(k) = CA^{k-1}B \tag{3}$$

with B an (n x m) matrix and C a (p x n) matrix. The ERA algorithm begins by defining the generalized Hankel matrix consisting of the discrete-time impulse responses for all input/output combinations. The algorithm then uses the singular value decomposition (SVD) to compute the A, B, and C matrices.

In this fashion, the ERA is applied to unsteady aerodynamic impulse responses to construct unsteady aerodynamic state-space models.

ROM Development Process

Unsteady Aerodynamic ROM

An outline of the improved simultaneous modal excitation ROM development process is as follows (see Figure 3):

1. Generate the number of functions (from a selected family) that corresponds to the number of structural mode shapes;

2. Apply the generated input functions simultaneously via one FUN3D execution; these responses are computed directly from the restart of a steady rigid FUN3D solution (not at a particular dynamic pressure); for the present results, Walsh functions are used as the input functions;

3. Using the simultaneous input/output responses, identify the individual impulse responses using the PULSE algorithm (within SOCIT);

4. Transform the individual impulse responses generated in Step 3 into an unsteady aerodynamic state-space system using the ERA (within SOCIT);

Once the unsteady aerodynamic state-space ROM is generated (Step 4), the state-space model is validated via comparison with FUN3D results (i.e., ROM results vs. full FUN3D solution results). Additional ROM enhancements and capabilities are described in greater detail in the references.[2]

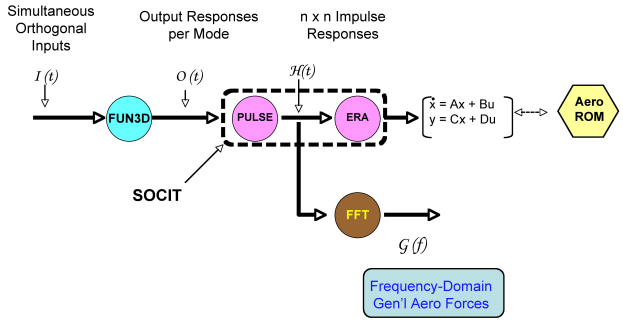

Fig. 3 Schematic of Unsteady Aerodynamic ROM Process.

An important difference between the original ROM process and the improved ROM process is stated in step (2) of the outline above. For the original ROM process, if a static aeroelastic condition existed, then a ROM was generated about a selected static aeroelastic condition. So a static aeroelastic condition of interest was defined (typically a dynamic pressure) and that static aeroelastic condition was computed using the aeroelastic CFD code as a restart from a converged steady, rigid solution. Once a converged static aeroelastic solution was obtained, the ROM process was applied about that condition. This implies that the resultant ROM is, of course, limited in some sense to the neighborhood of that static aeroelastic condition. Moving "too far away" from that condition could result in loss of accuracy.

The reason for generating ROMs in this fashion was because no method had been defined to enable the computation of a static aeroelastic solution using a ROM. Any ROMs generated in this fashion were, therefore, limited to the prediction of dynamic responses about a static aeroelastic solution including the methods by Kim et al[6] and by Raveh.[7] The improved ROM method, however, includes a method for generating a ROM directly from a steady, rigid solution. As a result, these improved ROMs can then be used to predict both static aeroelastic and dynamic solutions for any dynamic pressure. In order to capture a specific range of aeroelastic effects (previously obtained by selecting a particular dynamic pressure), the improved ROM method relies on the excitation amplitude to excite aeroelastic effects of interest. The details of the method for using a ROM for computing both static aeroelastic and dynamic solutions is pre-

sented in another reference by the first author.[2] For the present results, all responses were computed from the restart of a steady, rigid FUN3D solution, bypassing the need (and additional computational expense) to execute a static aeroelastic solution using FUN3D.

The Walsh functions that are applied simultaneously to the aeroelastic FUN3D code in order to excite all of the structural modes are generated based on the time step defined for the aeroelastic analysis. Typically, the full FUN3D static and dynamic aeroelastic solutions (each one generated separately) are computed using different time steps. The full FUN3D dynamic aeroelastic solution typically has the largest number of time steps so that sufficient cycles of the aeroelastic response are generated to provide adequate frequency information when post-processed. The size of the time steps for both the static and dynamic aeroelastic solutions are generally defined as large as possible for computationally efficient solutions. For the generation of the unsteady aerodynamic ROM, however, a time step is defined that is typically smaller (by an order of magnitude or so) so that relevant frequencies and associated dynamics are accurately resolved by the SOCIT tools due to Walsh input functions. For this reason, the single FUN3D solution to obtain the Walsh responses may take as long (CPU time) as a full FUN3D aeroelastic solution. However, the benefit of generating the unsteady aerodynamic ROM is that it can then be used to rapidly generate aeroelastic solutions at any other dynamic pressure and velocity (for a given Mach number) as well as any variation in structural parameters (modal damping, modal frequencies).

It should be mentioned that a full FUN3D aeroelastic solution for a given Mach number, dynamic pressure, and velocity consists of the computation of a steady rigid solution at that Mach number, followed by a static aeroelastic solution at that Mach number, dynamic pressure, and velocity, which is then followed by a dynamic aeroelastic solution at the same conditions. The steady rigid solution is computed rapidly as that solution is independent of aeroelastic responses and therefore independent of expensive mesh deformation iterations. The static aeroelastic response, restarted from the steady rigid solution, does require mesh deformations but an artificially high value of modal damping is used to accelerate the solution to a converged static aeroelastic response. The dynamic aeroelastic solution, restarted from the converged static aeroelastic solution, requires the most computational time due to the need for a certain number of cycles to accurately define dominant frequencies in the aeroelastic response. The computational cost of a ROM FUN3D solution (solution with Walsh functions applied) is on the order of a full FUN3D dynamic aeroelastic solution. Additional details regarding full FUN3D aeroelastic solutions can be found in the reference by Bartels et al.[18]

Structural Dynamic ROM

Normal modes analysis was performed with MSC.Nastran. Modal deflections were obtained by creating nodes at stations along the centerline of the vehicle at which the average of the circumferential outer mold line deflections at each axial station was computed using a wagon wheel interpolation connection to the outer mold line of the vehicle. The average deflection at the centerline node points was used to create the projection of the centerline modal deflections onto the CFD surface. The interpolation from the FEM node points to the CFD surface mesh points was accomplished by a spline fit, except at CFD mesh points beyond the first or last FEM node points where a quadratic extrapolation of the FEM data was used.

A total of forty-four flexible modes were used in the full FUN3D aeroelastic analyses of the Ares I-X vehicle, thirty-seven flexible modes were used in the full FUN3D aeroelastic analyses of the Ares I vehicle, while only thirteen flexible modes where used for the ROM aeroelastic analyses for both vehicles. The first thirteen flexible modes were used in the development of ROMs in order to be consistent with the number of modes being considered in related GNC analyses. For the majority of cases, no significant differences were identified either between the Ares I-X full FUN3D and ROM aeroelastic analyses or between the Ares I full FUN3D and ROM aeroelastic analyses.

Structural information from the Finite Element Analysis (MSC NASTRAN) such as generalized mass, generalized damping, and generalized frequencies (stiffness) is used to generate a state-space model of the structural dynamic system using MATLAB (see Figure 4). Once the ABCD matrices of the unsteady aerodynamic system are generated for a given Mach number, the unsteady aerodynamic system is combined with a set of ABCD matrices that define the structural dynamics. The combined use of these two systems leads to the simulation of the aeroelastic system as the structural and aerodynamic systems interact.

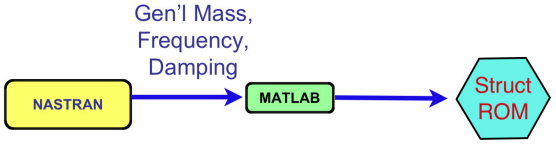

Fig. 4 Schematic of Structural Dynamic ROM Process.

Aeroelastic ROM

The MATLAB/SIMULINK environment from the Mathworks, Inc., is used to connect the state-space model of the unsteady aerodynamics and the state-space model of the structural dynamics into an aeroelastic reduced order model as shown in Figure 5. In addition, the structural dynamic model can be easily altered to simulate various values of structural damping and variations in modal frequencies. Simulation of the aeroelastic system with these variations provides a sensitivity study of the aeroelastic system to these parametric variations. For the computation of the aeroelastic root loci, the state-space ROM of the unsteady aerodynamic system and the state-space ROM of the structural dynamic system are mathematically combined into a single state-space model.

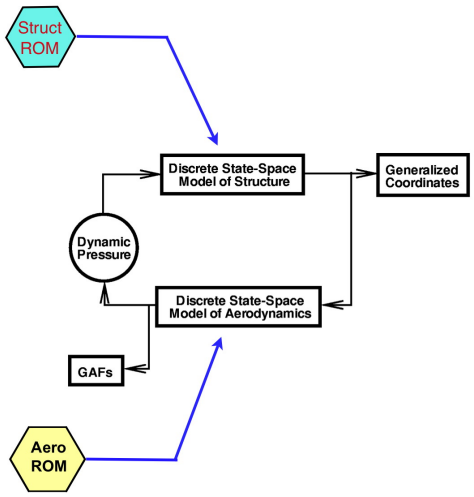

Fig. 5 Schematic of combined structural/unsteady aerodynamic ROM system, referred to as the Aeroelastic ROM.

Results

The goal of this section is to present a sample of results obtained in the process of generating and using an unsteady aerodynamic ROM and, subsequently, an aeroelastic ROM. Using these methods, aeroelastic results are then presented for the Ares I-X and the Ares I vehicles at various Mach numbers. It is important to reiterate that results presented are for analyses using the first thirteen flexible modes (no rigid-body modes).

When completed, the FUN3D Walsh solution is processed through MATLAB-based scripts that provide information regarding the error level of the subsequent unsteady aerodynamic ROM as compared to the full FUN3D Walsh solution. Samples of the time-domain responses due to the Walsh inputs for the full FUN3D solution and for the unsteady aerodynamic ROM are presented in Figure 6 for the first flexible mode and in Figure 7 for the second flexible mode. For the sake of clarity, discussions regarding the modes will focus on each individual flexible mode and not on the flexible mode pairs. That is, in some references, the first and second flexible mode comprise the first bending mode pair and are referred to as such.

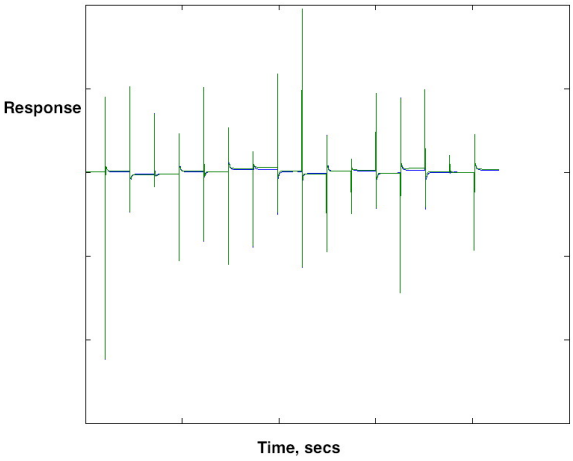

Fig. 6 Comparison of time-domain responses in the first flexible mode due to Walsh input functions for full FUN3D solution (blue) and for unsteady aerodynamic ROM (green).

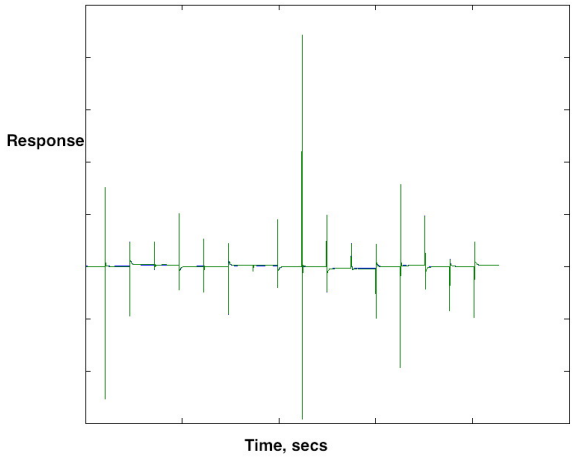

Fig. 7 Comparison of time-domain responses in the second flexible mode due to Walsh input functions for full FUN3D solution (blue) and for unsteady aerodynamic ROM (green).

The mean error and maximum percent error for the time-domain solutions for all thirteen flexible modes are presented in Figure 8. These errors are computed per mode (generalized coordinate) in order to better understand the impact of the error on the overall aeroelastic solution.

An analogous comparison of these responses is also viewed in the frequency domain. Presented in the up-

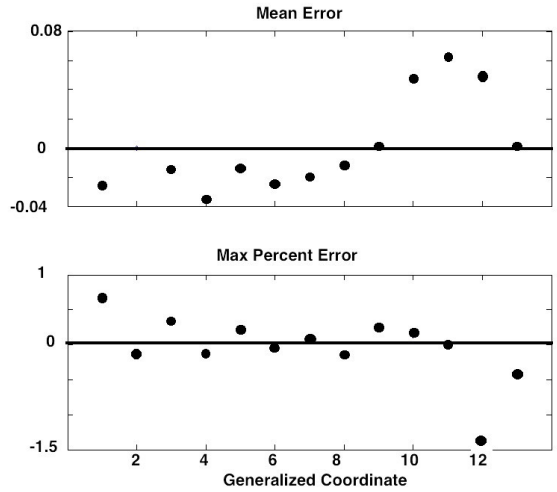

Fig. 8 The mean error and maximum percent error for the time-domain solutions.

per plot of Figure 9 is a comparison of the frequency content of the responses presented in Figure 6. Presented in the lower plot of Figure 9 is the frequency content of the input Walsh function for the first flexible mode.

Presented in Figure 10 are analogous plots corresponding to Figure 7 and the input Walsh function for the second flexible mode.

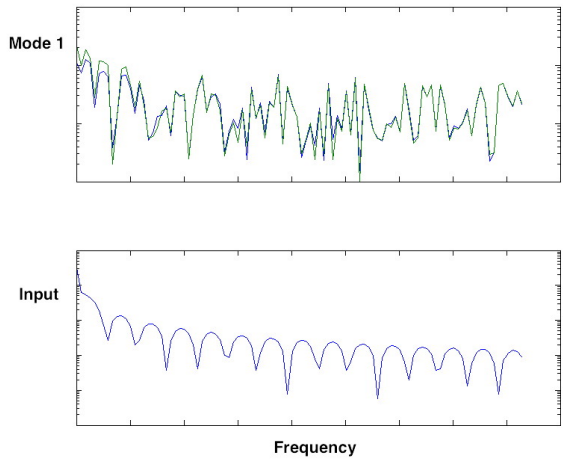

Fig. 9 (Upper plot): Comparison of frequency-domain responses in the first flexible mode due to Walsh input functions for full FUN3D solution (blue) and for unsteady aerodynamic ROM (green). (Lower plot): Frequency content of Walsh input function applied to first flexible mode.

Parameters within the PULSE and ERA algorithms that are used to generate the discrete-time state-space model are varied accordlingly until an acceptable error level is achieved. Upon achieving an acceptable error level (on the order of 1 percent or less in maximum percent error), the unsteady aerodynamic ROM

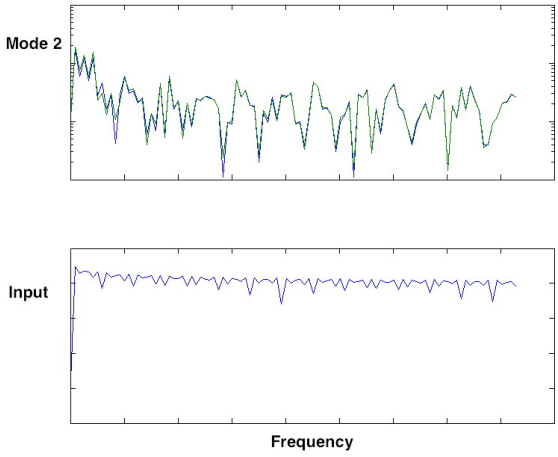

Fig. 10 (Upper plot): Comparison of frequency-domain responses in the second flexible mode due to Walsh input functions for full FUN3D solution (blue) and for unsteady aerodynamic ROM (green). (Lower plot): Frequency content of Walsh input function applied to second flexible mode.

is combined with the structural dynamic ROM to create the aeroelastic ROM. The aeroelastic ROM is then used to predict the aeroelastic response at various dynamic pressures, velocities, and structural dynamic parameter variations. These variations would require individual FUN3D solutions that could take on the order of days to compute while taking only seconds using the aeroelastic ROM.

Ares I-X

An important contribution of this effort is the ability to rapidly generate root locus plots of the aeroelastic behavior of the vehicle. Presented in Figure 11 is a root locus plot in terms of frequency versus damping ratio for the first thirteen flexible modes of the Ares I-X vehicle at a Mach number (M) of 0.5 and several dynamic pressures. Migration of the roots toward the right of the zero dynamic pressure value (Q=0 psi) indicates reduced damping (less stable); migration to the left of the zero dynamic pressure value indicates increased damping (more stable). Due to the structural symmetry of these launch vehicles, some of the flexible modes are very similar to each other. That is, the first flexible mode is a first-bending mode in the longitudinal axis while the second flexible mode is a first-bending mode in the lateral axis. As a result, some of the roots (symbols) in the root loci plots for some of these modes may be very close together or far apart, depending on the nature of the aeroelastic response. As can be seen, at this condition, both the first and second flexible modes exhibit a destabilizing effect as demonstrated by a migration of the roots to the right of the Q=0 values. A comparison of the full FUN3D aeroelastic response and the ROM aeroelastic

response at this Mach number and nominal dynamic pressure is presented as Figure 12 where good comparison between the two responses is evident.

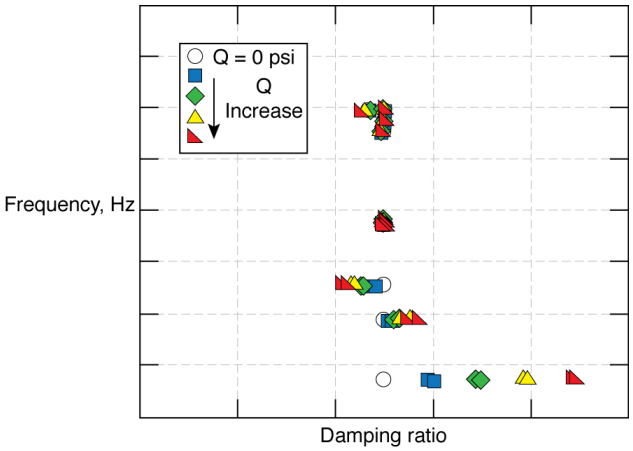

Fig. 11 Dynamic pressure root loci from aeroelastic ROM for nominal modal frequencies at M=0.5 for the Ares I-X vehicle.

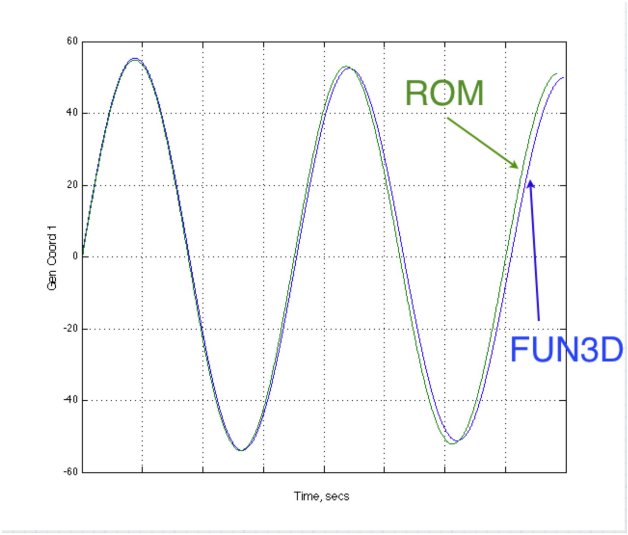

Fig. 12 Comparison of FUN3D and ROM aeroelastic responses at M=0.5 and nominal dynamic pressure for the first generalized coordinate (first elastic mode).

Via a simple modification of the structural dynamic ROM, the modal frequencies can be varied to account for a possible variation. Figure 13 presents the M=0.5 root locus plot for the condition where the modal frequencies have been increased by 10 percent (first and second modes) and by 20 percent (remaining modes). As can be seen, the effect of the increased frequencies is to provide a slight stiffening of the overall aeroelastic response. This slight stiffening is evident by comparing Figure 11 with Figure 13 showing a slightly decreased range of damping values for most of the modes where the scale is the same for both plots.

Figure 14 presents the root locus plot for the condition where the modal frequencies have been decreased by 10 percent (first and second modes) and by 20 percent (remaining modes). The decrease in the modal frequencies yields a slight softening of the aeroelastic response resulting in a greater destabilizing effect for the first two modes. This slight softening is evident by comparing Figure 11 with Figure 13 showing a slightly increased range of damping values for most of the modes where, again, the scale is the same for both plots. There is clearly a tendency towards destabilizing behavior at this Mach number.

At M=0.95, a different aeroelastic behavior is observed for the Ares I-X vehicle. As can be seen in Figure 15, there is an increase in stability with an increase in dynamic pressure at this Mach number for the nominal modal frequencies. For an increase in the modal frequencies identical to that performed previously, no detrimental effect is noticed at this Mach number as seen in Figure 16. However, for the case of decreased modal frequencies, reduced stability is observed for the twelfth flexible mode as indicated by the migration of the roots of that mode to the right of the Q=0 values, as seen in Figure 17. This indicates a potential sensitivity of that mode to slight variations in its modal frequency. Although not presented here, these aeroelastic ROM results compared very well with results from full FUN3D analyses at this condition.

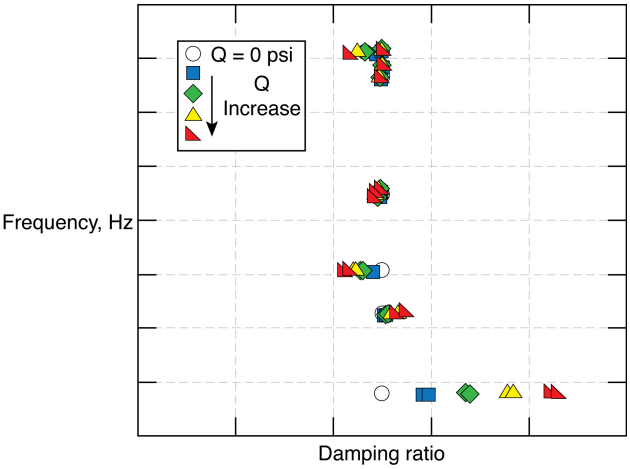

Fig. 13 Dynamic pressure root loci from aeroelastic ROM for increased modal frequencies at M=0.5 for the Ares I-X vehicle.

Analysis at a higher Mach number of 1.44 indicates that there is no effect on the stability of the vehicle due to variations in the modal frequencies. The result for nominal modal frequencies is shown in Figure 18, while the result for increased modal frequencies is shown in Figure 19 and that for decreased modal frequencies is shown in Figure 20. As can be seen, there is no migration of any of the roots to the right of the Q=0 values.

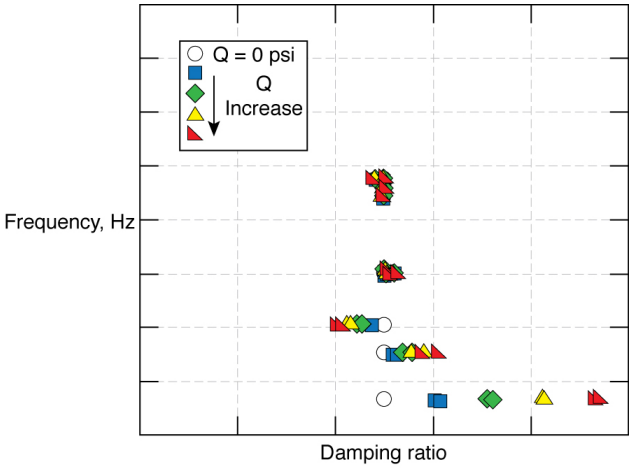

Fig. 14 Dynamic pressure root loci from aeroelastic ROM for decreased modal frequencies at M=0.5 for the Ares I-X vehicle.

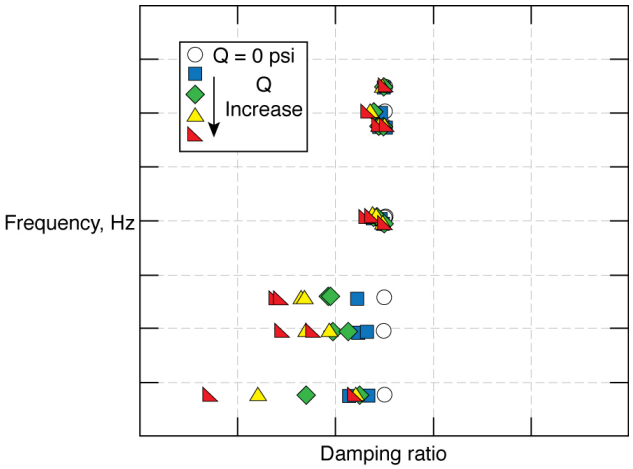

Fig. 15 Dynamic pressure root loci from aeroelastic ROM for nominal modal frequencies at M=0.95 for the Ares I-X vehicle.

Ares I

Unsteady aerodynamic and aeroelastic ROMs also were generated for the Ares I vehicle at several Mach numbers and for a specific variation in the structural dynamics of the vehicle. This structural dynamic variation is due in part to the inclusion of a dual-plane Thrust Oscillation Isolator (TOI) modified model and it results in a different structural dynamic representation than the baseline Ares I vehicle model. Although the intent of the TOI system is to reduce vibrations associated with the propulsion system, the TOI system as modeled actually introduces additional flexibility that has a detrimental effect on aeroelastic stability. In addition to the flexibility introduced by the TOI system, the baseline Ares I vehicle is more flexible than the Ares I-X vehicle. In this section, results are presented for the M=1.00 condition.

Presented in Figure 21 is a comparison of the full

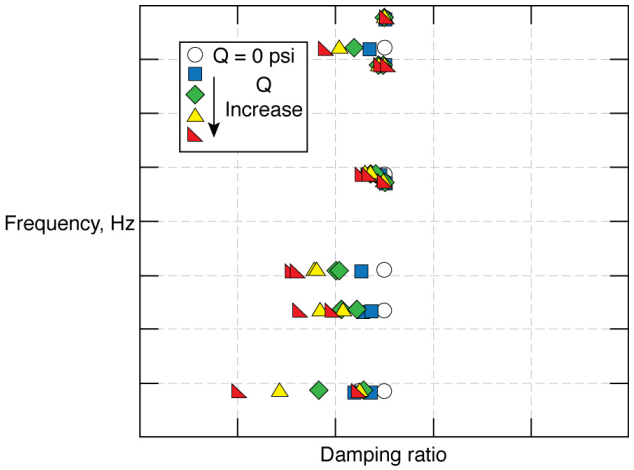

Fig. 16 Dynamic pressure root loci from aeroelastic ROM for increased modal frequencies at M=0.95 for the Ares I-X vehicle.

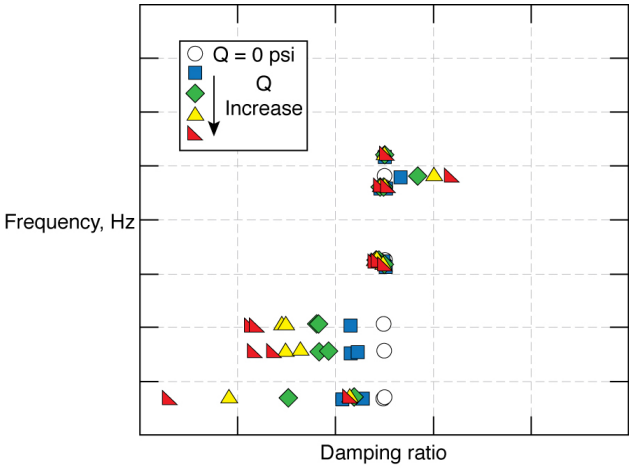

Fig. 17 Dynamic pressure root loci from aeroelastic ROM for decreased modal frequencies at M=0.95 for the Ares I-X vehicle.

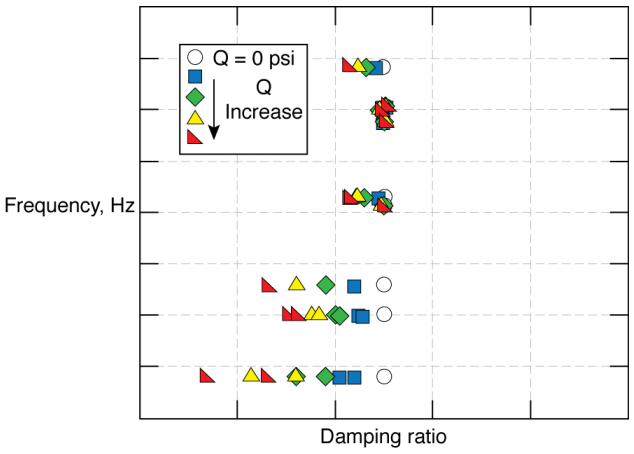

Fig. 18 Dynamic pressure root loci from aeroelastic ROM for nominal modal frequencies at M=1.44 for the Ares I-X vehicle.

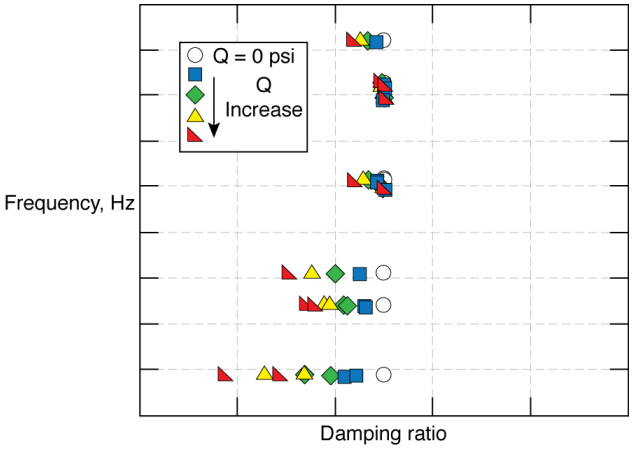

Fig. 19 Dynamic pressure root loci from aeroelastic ROM for increased modal frequencies at M=1.44 for the Ares I-X vehicle.

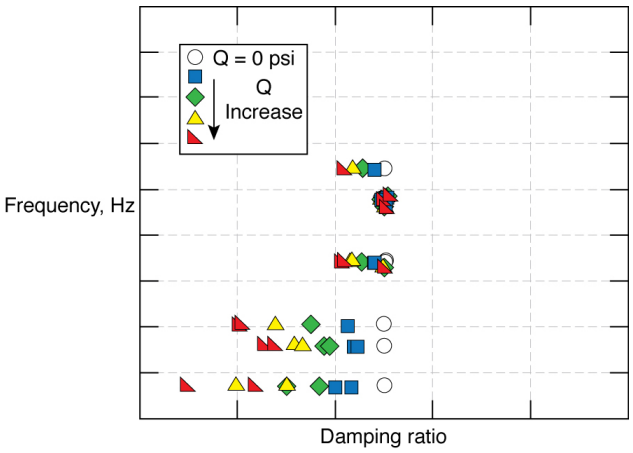

Fig. 20 Dynamic pressure root loci from aeroelastic ROM for decreased modal frequencies at M=1.44 for the Ares I-X vehicle.

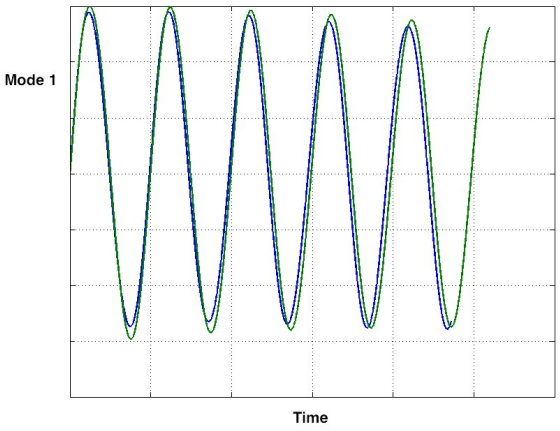

Fig. 21 Comparison of full FUN3D and ROM aeroelastic responses at M=1.00 for the first flexible mode of the baseline Ares-I vehicle (ROM-Green; FUN3D-Blue).

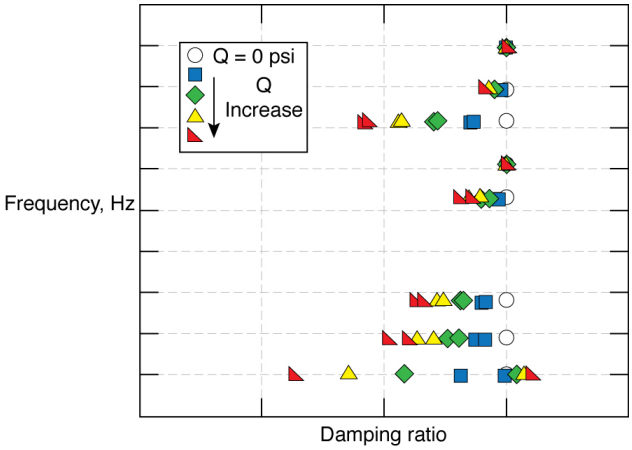

Fig. 22 Dynamic pressure root loci from aeroelastic ROM at M=1.00 for the baseline Ares I vehicle.

FUN3D and the ROM aeroelastic responses at M=1.00 for the first flexible mode of the baseline Ares I vehicle. As can be seen, the comparison is very good with the ROM result only slightly less stable (less damping) than the full FUN3D solution.

The root loci at M=1.00 for the baseline Ares I vehicle is presented in Figure 22. For this version of the vehicle, it can be seen that most of the aeroelastic roots migrate to the left of the Q=0 points, indicating increased damping, and, therefore, increased stability. However, for the first mode there appears to be a root migration to the right, indicating decrease damping and, therefore, decreased stability.

Presented in Figure 23 is a comparison of the full FUN3D and the ROM aeroelastic responses at M=1.00 for the first flexible mode of the TOI-modified Ares I vehicle. Once again, the comparison is very good with the ROM result only slightly less stable (less damping) than the full FUN3D solution.

Finally, the root loci at M=1.00 for the TOI-modified Ares I vehicle is presented in Figure 24. By comparing this root loci with that for the baseline Ares I vehicle, it can be seen that modification of the Ares I vehicle to include the TOI system tends to reduce the stability of the first flexible mode as indicated by the migration of the roots of the first flexible mode to the right of the Q=0 point beyond the point seen in Figure 22. The rapid assessment of this reduced-stability condition was an important contribution of the ROM methodology as applied to these vehicles. Subsequent full FUN3D aeroelastic solutions confirmed these ROM aeroelastic results.

Concluding Remarks

Methods for generating unsteady aerodynamic reduced-order models (ROMs) and aeroelastic ROMs have been presented. These methods were applied towards the development of unsteady aerodynamic, structural dynamic, and aeroelastic ROMs for the Ares

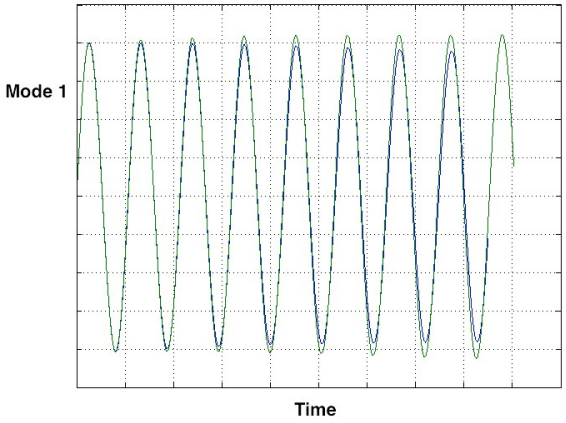

Fig. 23 Comparison of full FUN3D and ROM aeroelastic responses at M=1.00 for the first flexible mode of the TOI-modified Ares-I vehicle (ROM-Green; FUN3D-Blue).

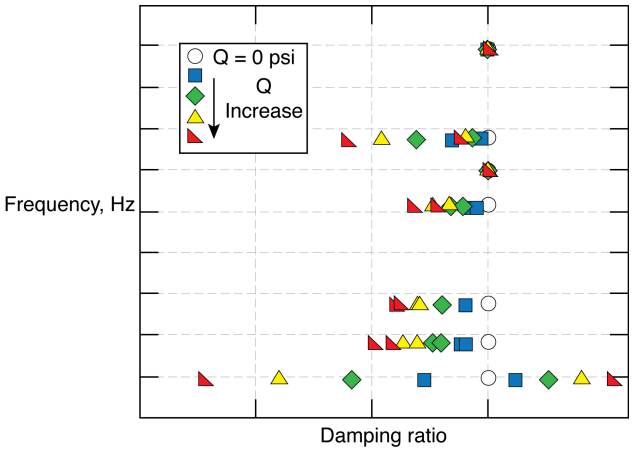

Fig. 24 Dynamic pressure root loci from aeroelastic ROM at M=1.00 for the TOI-modified Ares I vehicle.

I-X and Ares I launch vehicles in order to quickly generate aeroelastic response information. A sample of results presented included error minimization techniques, comparison of aeroelastic responses for the full FUN3D solution versus the aeroelastic ROM solution, and root locus plots for parametric variations of modal frequency. The ability to rapidly generate aeroelastic root loci as a function of dynamic pressure at a given Mach number provided valuable insight regarding the nature of the aeroelastic response of these launch vehicles. Of particular significance is the fact that aeroelastic interactions amongst the various modes for launch vehicles is unlike the typical aeroelastic interactions of lifting surfaces. Whereas the aeroelastic interactions of a lifting surface may reveal a coalescence of two modes originally at different frequencies, the aeroelastic interactions for these launch vehicles consist of a coupling of modes at very nearly the same frequency with minimal variation in frequency for all modes as a function of dynamic pressure. This should not be surprising as lauch vehicles are not lifting surfaces. Another important contribution of this ROM methodology was the identification of reduced aeroelastic stability of the Ares I vehicle with the TOI system at a transonic Mach number. The methods were shown to be a powerful tool to enable the rapid assessment of aeroelastic behavior of this class of launch vehicles.

Acknowledgement

This work was performed in support of and funded by the Ares I-X and the Ares I Program Offices.

References

[1]Silva, W. A., "Simultaneous Excitation of Multiple-Input/Multiple-Output CFD-Based Unsteady Aerodynamic Systems," *Journal of Aircraft*, Vol. 45, No. 4, July-August 2008, pp. 1267–1274.

[2]Silva, W. A., "Recent Enhancements to the Development of CFD-Based Aeroelastic Reduced Order Models," *48th AIAA/ASME/ASCE/AHS/ASC Structures, Structural Dynamics, and Materials Conference*, No. AIAA Paper No. 2007-2051, Honolulu, HI, April 23-26 2007.

[3]Silva, W. A., "Identification of Nonlinear Aeroelastic Systems Based on the Volterra Theory: Progress and Opportunities," *Journal of Nonlinear Dynamics*, Vol. 39, Jan. 2005.

[4]Silva, W. A. and Bartels, R. E., "Development of Reduced-Order Models for Aeroelastic Analysis and Flutter Prediction Using the CFL3Dv6.0 Code," *Journal of Fluids and Structures*, No. 19, 2004, pp. 729–745.

[5]Beran, P. S. and Silva, W. A., "Reduced-Order Modeling: New Approaches for Computational Physics," *Presented at the 39th AIAA Aerospace Sciences Meeting, 8-11 January 2001, Reno,NV*, January 2001.

[6]Kim, T., Hong, M., Bhatia, K. G., and SenGupta, G., "Aeroelastic Model Reduction for Affordable Computational Fluid Dynamics-Based Flutter Analysis," *AIAA Journal*, Vol. 43, 2005, pp. 2487–2495.

[7]Raveh, D. E., "Identification of Computational-Fluid-Dynamic Based Unsteady Aerodynamic Models for Aeroelastic Analysis," *Journal of Aircraft*, Vol. 41, June 2004, pp. 620–632.

[8]Silva, W. A., Beran, P. S., Cesnik, C. E. S., Guendel, R. E., Kurdila, A., Prazenica, R. J., Librescu, L., Marzocca, P., and Raveh, D., "Reduced-Order Modeling: Cooperative Research and Development at the NASA Langley Research Center," *CEAS/AIAA/ICASE/NASA International Forum on Aeroelasticity and Structural Dynamics*, June 2001.

[9]Silva, W. A., "Reduced-Order Models Based on Linear and Nonlinear Aerodynamic Impulse Responses," *CEAS/AIAA/ICASE/NASA International Forum on Aeroelasticity and Structural Dynamics*, June 1999.

[10]Silva, W. A., *Discrete-Time Linear and Nonlinear Aerodynamic Impulse Responses for Efficient CFD Analyses*, Ph.D. thesis, College of William & Mary, December 1997.

[11]Silva, W. A., "Application of Nonlinear Systems Theory to Transonic Unsteady Aerodynamic Responses," *Journal of Aircraft*, Vol. 30, 1993, pp. 660–668.

[12]Raveh, D. E., Levy, Y., and Karpel, M., "Aircraft Aeroelastic Analysis and Design Using CFD-Based Unsteady Loads," *41st Structures, Structural Dynamics, and Materials Conference*, No. 2000-1325, Atlanta, GA, April 2000.

[13]Juang, J.-N. and Pappa, R. S., "An Eigensystem Realization Algorithm for Modal Parameter Identification and Model Reduction," *Journal of Guidance, Control, and Dynamics*, Vol. 8, 1985, pp. 620–627.

[14]"Registered Product of the MathWorks, Inc." .

[15]Biedron, R. T. and Thomas, J., "Recent Enhancements to the FUN3D Flow Solver for Moving-Mesh Applications," *47th AIAA Aerospace Sciences Meeting*, No. 2009-1360, Orlando, FL, Jan. 5-8 2009.

[16]Juang, J.-N., Phan, M., Horta, L. G., and Longman, R. W., "Identification of Observer/Kalman Filter Markov Parameters: Theory and Experiments," *Journal of Guidance, Control, and Dynamics*, Vol. 16, 1993, pp. 320–329.

[17]Juang, J.-N., *Applied System Identification*, Prentice-Hall PTR, 1994.

[18]Bartels, R., Chwalowski, P., Massey, S., Vatsa, V., Heeg, J., Mineck, R., and Wieseman, C., "Computational Aeroelastic Analysis of the Ares Crew Launch Vehicle During Ascent," *28th AIAA Applied Aerodynamics Conference*, No. 2010-4374, Chicago, IL, June 28 - July 1 2010.